Nematode ascarosides attenuate mammalian type 2 inflammatory responses

Kenta Shinoda[a,1], Andrea Choe[b,1], Kiyoshi Hirahara[a,c,1], Masahiro Kiuchi[a], Kota Kokubo[a], Tomomi Ichikawa[a], Jason S. Hoki[d], Akane S. Suzuki[e], Neelanjan Bose[d], Judith A. Appleton[f], Raffi V. Aroian[g], Frank C. Schroeder[d], Paul W. Sternberg[b,2], and Toshinori Nakayama[a,h,2]

[a]Department of Immunology, Graduate School of Medicine, Chiba University, Chuo-ku, Chiba 260-8670, Japan; [b]Division of Biology and Biological Engineering, California Institute of Technology, Pasadena, CA 91125; [c]Japan Agency for Medical Research and Development (AMED)-PRIME, AMED, Chuo-ku, Chiba 260-8670, Japan; [d]Boyce Thompson Institute, Department of Chemistry and Chemical Biology, Cornell University, Ithaca, NY 14853; [e]Department of Medical Immunology, Graduate School of Medicine, Chiba University, Chuo-ku, Chiba 260-8670, Japan; [f]Baker Institute for Animal Health, Cornell University, Ithaca, NY 14853; [g]Program in Molecular Medicine, University of Massachusetts Medical School, Worcester, MA 01605; and [h]Japan Agency for Medical Research and Development (AMED)-CREST, AMED, Chuo-ku, Chiba 260-8670, Japan

Contributed by Paul W. Sternberg; received May 13, 2021; accepted December 28, 2021; reviewed by Rick Maizels and Steven Ziegler

Mounting evidence suggests that nematode infection can protect against disorders of immune dysregulation. Administration of live parasites or their excretory/secretory (ES) products has shown therapeutic effects across a wide range of animal models for immune disorders, including asthma. Human clinical trials of live parasite ingestion for the treatment of immune disorders have produced promising results, yet concerns persist regarding the ingestion of pathogenic organisms and the immunogenicity of protein components. Despite extensive efforts to define the active components of ES products, no small molecules with immune regulatory activity have been identified from nematodes. Here we show that an evolutionarily conserved family of nematode pheromones called ascarosides strongly modulates the pulmonary immune response and reduces asthma severity in mice. Screening the inhibitory effects of ascarosides produced by animal-parasitic nematodes on the development of asthma in an ovalbumin (OVA) murine model, we found that administration of nanogram quantities of ascr#7 prevented the development of lung eosinophilia, goblet cell metaplasia, and airway hyperreactivity. Ascr#7 suppressed the production of IL-33 from lung epithelial cells and reduced the number of memory-type pathogenic Th2 cells and ILC2s in the lung, both key drivers of the pathology of asthma. Our findings suggest that the mammalian immune system recognizes ascarosides as an evolutionarily conserved molecular signature of parasitic nematodes. The identification of a nematode-produced small molecule underlying the well-documented immunomodulatory effects of ES products may enable the development of treatment strategies for allergic diseases.

asthma | mouse model | nematode | small molecules | ascarosides

Parasitic nematodes are associated with almost all groups of vertebrates, and nearly one-third of the human population is infected with these helminths (1). Their omnipresence is in part due to their ability to modulate host immune responses to prevent immune attack and expulsion (2). The elimination of nematode infections has been proposed as a possible cause of the increased incidence of autoimmune disorders and allergic diseases in developed countries (3), based on epidemiological data showing a correlation between the decline in helminth infection and the rise in allergic and autoimmune diseases, including asthma, multiple sclerosis (MS), type 1 diabetes, and inflammatory bowel diseases (IBDs) (4).

The administration of live nematodes or their excretory/secretory (ES) products has shown therapeutic effects across a wide range of animal models for these immune disorders (5–8). The US Food and Drug Administration recently approved live helminth administration as an investigational drug for the treatment of immune disorders, and relevant human clinical trials are ongoing (9). Despite mounting evidence that helminths have significant therapeutic potential, we do not yet have a comprehensive understanding of the molecules that underlie their immunomodulatory effects; and, in particular, the possible relevance of low-molecular-weight components of ES products has remained largely unexplored.

A wide range of nematodes, including many parasitic species, produce ascarosides, a family of small-molecule signals based on glycosides of the dideoxysugar ascarylose (10). Ascarosides have not yet been identified in any other animal phylum, suggesting that they may be a nematode-specific class of small molecules (*SI Appendix*, Fig. S1*A*). The first ascaroside-based signaling molecules were identified in the free-living model nematode

Significance

Animal proof-of-concept studies have shown that roundworms have a protective effect against immune-dysregulated disorders, but it has been difficult to study in human trials without individual nematode-derived molecules to develop and test. We discovered that ascarosides, molecules that are secreted by diverse nematodes, suppress asthma in a rodent model via modulation of expression of *Il33*, a key epithelial cytokine for induction of type 2 immunity, in addition to decreasing memory-type pathogenic Th2 cells and ILC2s and increasing the *Il10*-expressing subpopulation of interstitial macrophages in the lung. Thus, ascarosides suppress type 2 immune response by affecting both innate and adaptive immunity and could define a potent class of small molecule drugs to treat allergic airway diseases.

Author contributions: K.S., A.C., K.H., F.C.S., P.W.S., and T.N. designed research; K.S., A.C., M.K., K.K., T.I., J.S.H., A.S.S., N.B., J.A.A., and R.V.A. performed research; J.S.H., J.A.A., R.V.A., and F.C.S. contributed new reagents/analytic tools; K.S., K.H., M.K., T.I., A.S.S., N.B., F.C.S., and T.N. analyzed data; and K.S., A.C., K.H., F.C.S., and T.N. wrote the paper.

Reviewers: R.M., University of Glasgow; and S.Z., Benaroya Research Institute at Virginia Mason.

Competing interest statement: The patent rights related to the results reported here have been licensed to Holoclara, Inc., a privately held company that has been pursuing ascr#7-related compounds as potential therapeutics since its founding in 2017. A.C., P.W.S., and F.C.S. are cofounders and stockholders of Holoclara, Inc., and A.C. is the company's chief executive officer. The patent rights have also been licensed to Ascribe Bioscience, Inc., a privately held company where F.C.S. is a cofounder and a stockholder. While most of the studies reported here predate the founding of the company, Holoclara, Inc. funded part of the work. Holoclara, Inc. is not publicly traded and there are no plans for an initial public offering.

See online for related content such as Commentaries.

[1]K.S., A.C., and K.H. contributed equally to this work.

[2]To whom correspondence may be addressed. Email: pws@caltech.edu or tnakayama@faculty.chiba-u.jp.

This article contains supporting information online at http://www.pnas.org/lookup/suppl/doi:10.1073/pnas.2108686119/-/DCSupplemental.

Published February 24, 2022.

Caenorhabditis elegans (11, 12). Ascarosides regulate almost every aspect of *C. elegans* life history, including diapause (dauer) induction, aging, mate finding, and aggregation (11, 12). Subsequently, ascarosides have been shown to be detected by organisms other than nematodes, such as nematophagous fungi that set traps to capture and digest nematodes (13). The perception of ascarosides is sufficient to trigger trap formation in these fungi, demonstrating their longstanding evolutionary association with nematodes. Furthermore, ascarosides produced by plant-pathogenic nematodes have been shown to trigger innate immune responses in monocot and dicot plants (14). Cumulatively, these findings suggest that ascarosides represent a nematode-specific molecular signature that is recognized and interpreted by nematode predators and hosts across multiple kingdoms.

In this study, we collected ES products from the gut-resident, rodent-parasitic nematode *Nippostrongylus brasiliensis*. Previous studies showed that the administration of *N. brasiliensis* ES (NES) products fully inhibits the development of airway hyperresponsiveness (AHR) in the ovalbumin (OVA) murine model of asthma (15). Specifically, NES products substantially prevented lung eosinophilia, mucus production, and resistance to airflow. Notably, it was found that heat-treated or proteinase K–treated NES mimicked the full effect of untreated NES products in reducing lung eosinophilia and OVA-specific IgG in serum. Therefore, we hypothesized that the therapeutic effect of NES products may be due to the presence of specific small molecules that may in part be bound to secreted proteins, explaining the activity of heat- or proteinase K–treated NES. To test this hypothesis, we isolated the small molecule fraction of heat-treated NES (small molecule ES [smES]) products via filtration through a 3-kDa filter and found that smES products strongly suppresses OVA-induced allergic immune responses. Parallel chemical analyses of several other mammalian parasitic nematodes confirmed the presence of specific ascarosides in smES products of all tested species. Next, we tested synthetic samples of ascarosides and found that ascr#7, a compound produced by *N. brasiliensis* and other parasitic species, markedly inhibited the development of allergic airway inflammation, comparable to the full effect of smES products. Mechanistically, we found that ascr#7 administration attenuated IL-33 production from lung epithelial cells and suppressed the proliferation of memory-type IL-5–producing pathogenic T helper 2 (Th2) cells and type 2 innate lymphoid cells (ILC2s) in the lung, both key drivers for the pathology of asthma. We thus demonstrate that ascarosides have an immunomodulatory role that attenuates OVA-induced allergic inflammation in a murine model.

Results

Sensitization with NES-Derived Small Molecules Inhibits the Development of OVA-Induced Airway Inflammation. We first tested whether smES, derived from mixed-gender, adult *N. brasiliensis* had the capacity to suppress OVA-specific allergic responses in mice. smES was administered together with OVA/alum intraperitoneally at days 0 and 14 of a sensitization period, followed by intranasal OVA challenge at day 24 (Fig. 1*A*). Mice were then evaluated for the development of OVA-specific allergic responses at day 30, at which time the bronchoalveolar lavage (BAL) fluid was harvested and examined for the infiltration of inflammatory cells.

Eosinophil and lymphocyte infiltration was significantly decreased in mice sensitized with OVA/alum plus smES compared to OVA-sensitized control mice (Fig. 1*B*). Histological analyses revealed the absence of inflammatory cell infiltration in the lungs of mice that received neither OVA sensitization nor challenge (Fig. 1 *C*, *Right*). Challenge with OVA resulted in substantial infiltration of mononuclear cells into the perivascular and peribronchiolar regions, whereas mice sensitized with OVA/alum plus smES showed significantly lower levels of cell infiltration in the lung (Fig. 1 *C*, *Left* and *Middle*). Enhanced mucus production was detected in bronchioles of asthmatic lungs of OVA-sensitized control mice, whereas ameliorated mucus production was observed for mice sensitized with OVA/alum plus smES (Fig. 1*D*). Furthermore, mice sensitized with OVA/alum plus smES showed a decreased expression of mucus production–related genes, including *Muc5ac*, *Gob-5*, and *Muc5b*, in the lungs compared to mice sensitized with OVA/alum alone (Fig. 1*E*). These results show that smES has potent inhibitory activity on OVA-induced allergic airway inflammation.

Ascaroside-Containing smES Fractions Suppress OVA-Induced Allergic Airway Inflammation. To identify specific molecules in smES that suppress OVA-induced allergic airway inflammation, we chromatographically fractionated smES and tested the resulting eight fractions in the OVA murine model. Infiltration with eosinophils and lymphocytes was significantly reduced in mice sensitized with OVA/alum with addition of fraction 5 or 8 (Fig. 2*A*). In contrast, mice sensitized with OVA/alum plus fraction 1 exhibited significantly increased lymphocyte and macrophage infiltration (Fig. 2*A*). Analysis via high-performance liquid chromatography coupled to mass spectrometry (HPLC-MS) using a sensitive and selective tandem-MS screening method (16) revealed that fraction 5 contained the ascarosides ascr#1 and ascr#7, whereas fraction 8 contained ascr#3 and ascr#10 (Fig. 2*B*). These findings echo those of previous studies that reported the presence of ascr#3, ascr#7, and ascr#10 in adult smES and additionally revealed the presence of ascr#1, which had not been reported previously as a component of smES (10). Importantly, ascarosides were only detected in fractions 5 and 8, which reduced infiltration with eosinophils and lymphocytes, but not in any of the other tested fractions.

Production of ascr#1 and ascr#7 Is Widespread among Mammalian Parasitic Nematodes. We next examined whether ascarosides are also produced by other helminthic nematode species reported to have immunosuppressive effects in humans or animals, including *Trichuris suis*, *Ancylostoma ceylanicum*, *Heligmosomoides polygyrus*, and *Trichinella spiralis*. Targeted HPLC-MS analysis of the smES and small-molecule worm body extracts revealed the presence of ascr#1 in smES of all four species, accompanied by smaller amounts of ascr#7 (*SI Appendix*, Table S1). In contrast to *N. brasiliensis*, ascr#3 or ascr#10 were not consistently detected in smES samples from these four species, although ascr#10 was present in the worm body extracts of *T. suis*, *A. ceylanicum*, and *H. polygrus*. These results suggested that ascr#1 and/or ascr#7 may be responsible for part of the immunosuppressive activity of ES products from these species.

Synthetic Ascarosides Suppress OVA-Induced Allergic Airway Inflammation. Next, we tested whether synthetic samples of the four ascarosides identified in the active *N. brasiliensis* fractions affect OVA-induced allergic airway inflammation. Our HPLC-MS analyses indicated that concentrations of ascarosides in smES are low, amounting to roughly 0.5 to 1 nmol in the quantity of smES used per treatment, and we thus used 1 nmol of ascaroside (~0.3 μg) per treatment for testing synthetic samples. The coadministration of ascr#1, ascr#3, ascr#7, or smES with OVA/alum reduced eosinophilic infiltration in the BAL fluid compared to solvent control with OVA/alum (Fig. 2*C*), whereas coadministration of ascr#10 with OVA/alum had no effect on the infiltration of eosinophils in the BAL fluid. The number of mononuclear cells infiltrating the perivascular and peribronchiolar regions of the lungs was significantly reduced by coadministration of ascr#7, but not with the other three tested ascarosides (Fig. 2*D*). The number of infiltrating $CD11b^{+}Siglec\text{-}F^{+}$ eosinophils was reduced in the lungs of mice sensitized with OVA/alum plus ascr#7 (Fig. 2*E*). AHR was attenuated in mice sensitized with OVA/alum plus ascr#3

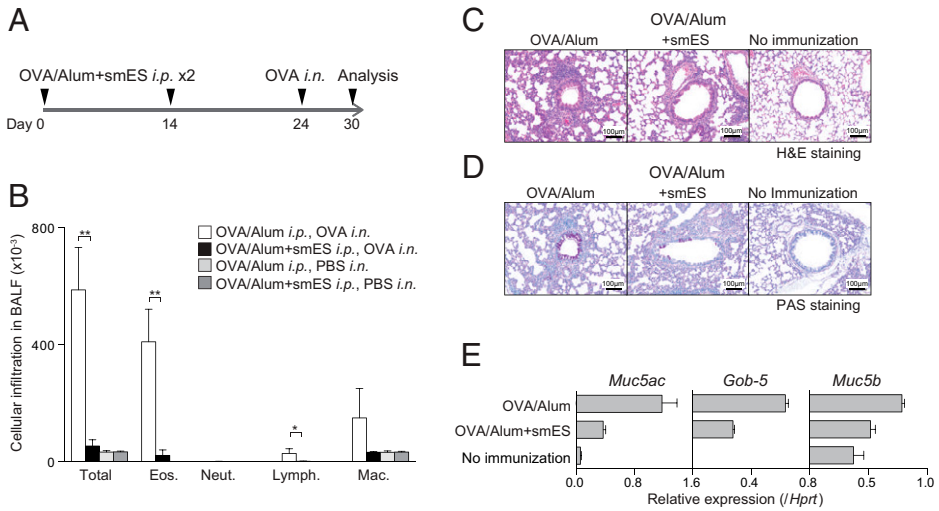

Fig. 1. *N. brasiliensis* smES products suppress OVA-induced allergic immune responses. (*A*) C57BL/6 mice were immunized with smES or control plus OVA in alum on days 0 and 14 and then challenged with the intranasal (i.n.) administration of OVA or PBS. Six days after the challenge, OVA-induced inflammation in the lung was analyzed. (*B*) Absolute numbers of eosinophils (Eos.), neutrophils (Neut.), lymphocytes (Lymph.), and macrophages (Mac.) in the BAL fluid are shown. These results were obtained using values from cell counting, the percentages of the cells, the total cell number per milliliter, and the volume of the BAL fluid recovered. Data from one experiment are representative of four independent experiments. (*C* and *D*) Lungs were fixed and stained with (*C*) H&E or (*D*) PAS. (Scale bars, 100 mm.) (*E*) Total RNA was prepared from the lung tissue, and the expression of *Gob5*, *Muc5ac*, and *Muc5b* was determined by quantitative RT-PCR. Relative intensities (*Hprt*; mean of three samples) are shown with SD. Mean values from four mice (*B*) per group are shown with SD. $*P < 0.05$, $**P < 0.01$.

and ascr#7 as compared to those in the control group (Fig. 2*F*). Both mucus hyperproduction and goblet cell metaplasia, as assessed by periodic acid-Schiff (PAS) staining, were ameliorated in the bronchioles of mice sensitized with OVA/alum plus ascr#7 (Fig. 2*G*). To determine whether ascr#7 can directly suppress allergic airway inflammation, mice were primed with OVA/alum without ascr#7, and instead ascr#7 was administered during the challenge phase (*SI Appendix*, Fig. S2*A*). Numbers of infiltrated inflammatory cells in the BAL fluid and lung histology showed no significant differences between groups of mice with or without administration of ascr#7 during the challenge phase (*SI Appendix*, Fig. S2 *B–D*).

Next we tested the effect of ascr#7 in a bona fide model for allergic airway inflammation, using house dust mite (HDM) antigen. Repeated exposure of mice to HDM antigen induced lung infiltration with inflammatory cells, accompanied by goblet cell metaplasia, which was significantly ameliorated by administration of ascr#7 (*SI Appendix*, Fig. S3). Taken together, these results show that ascr#7 has a strong inhibitory effect on both OVA-induced and HDM-induced allergic airway inflammation. Ascr#1 and ascr#3 may contribute to this effect in combination with ascr#7 as components of smES. Notably, ascr#1 and ascr#7 were present in all of the analyzed immunosuppressive nematode species.

Ascaroside Structure–Activity Relationships in the OVA AHR Assay. We then examined whether other, structurally different ascarosides not detected in the analyzed mammalian parasitic species also attenuated the OVA-induced allergic AHR. We selected ascr#9, which is similar to ascr#7 but has a slightly shorter (five-carbon) side chain that lacks a double bond, as well as pasc#9 and dasc#1, two ascarosides of similar polarity but with very different chemical structures (Fig. 2*B*). Comparing these three ascarosides to ascr#1 and ascr#7 in the OVA-induced airway inflammation, we found that the coadministration of ascr#1, ascr#7, and to a lesser extent dasc#1 significantly reduced total numbers of infiltrating leukocytes, whereas the other tested ascarosides had no effect (Fig. 2*H*). A significant decrease in the absolute number of eosinophils and lymphocytes was observed only in the ascr#1- and ascr#7-treated mice. These results indicate that, while ascarosides are commonly produced by mammalian parasitic nematodes, ascr#1 and ascr#7 specifically have immunosuppressive activity in OVA-induced airway inflammation, and ascarosides that only occur in other nematode species (e.g., dasc#1 and pasc#9) or are not widespread among mammalian parasitic nematodes are less likely to be active.

The Administration of Ascr#7 Decreases the Number of ST2^{hi} Th2 Cells. To characterize the immune cells affected by the administration of ascr#7, we generated single-cell RNA-seq (scRNA-seq) profiles with CD45^{+} immune cells collected from the lungs of mice sensitized with OVA/alum only or OVA/alum plus ascr#7 followed by intranasal OVA challenge (Fig. 1*A*). Overall, we identified 23 clusters in an unbiased manner based on differentially expressed genes and inferred cluster identities based on the expression of marker genes (Fig. 3*A* and *SI Appendix*, Fig. S4*A*). Ascr#7 treatment resulted in a decrease in the number of Th2 cells and ILCs in inflamed lungs (Fig. 3*B*). Uniform manifold approximation and projection (UMAP) plots revealed a decreased number of *Gata3*-expressing Th2 cells in the lungs of mice sensitized with OVA/alum plus ascr#7 (Fig. 3 *C*, *Upper*). The IL-5 producing subpopulation of Th2 cells is key for the induction of eosinophilic inflammation and characterized by the expression of ST2, a component of the IL-33 receptor encoded by *Il1rl1* (17). Indeed, *Il1rl1*-expressing Th2 cells, which have the ability to produce large amounts of IL-5 by the combined stimulation of the T cell receptor (TCR) and IL-33, were significantly decreased among Th2 cells in the lungs of mice sensitized with OVA/alum plus ascr#7 (Fig. 3 *C*, *Lower* and *D*) (17). Taken together with the results of the scRNA-seq analysis, these findings indicate that ascr#7 suppressed type 2 immune responses via a reduction in the number of *Il1rl1*-expressing Th2 cells.

Ascr#7 Suppresses Both Innate and Adaptive Type 2 Immunity. We next tested whether ST2-expressing Th2 cells were decreased after OVA/alum immunization plus ascr#7 in the spleen (*SI Appendix*, Fig. S5*A*). Numbers of CD44^{hi}ST2^{+} Th2 cells were significantly decreased in the spleen of ascr#7-treated mice on

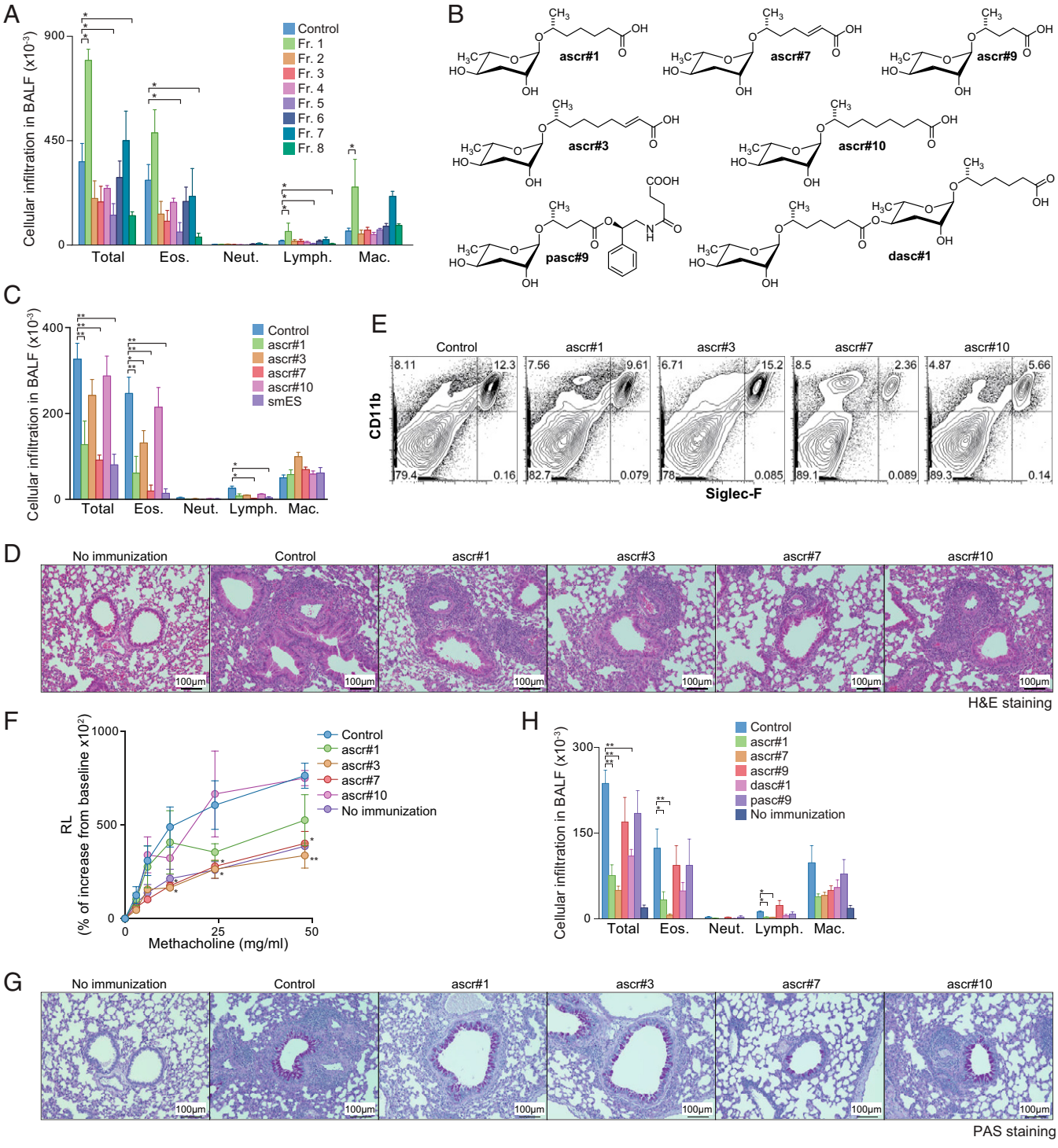

Fig. 2. OVA-induced allergic immune responses were attenuated by ascarosides. (*A*) *N. brasiliensis* smES was chromatographically fractionated, and the resulting eight fractions (fractions 1 through 8) were assayed using the protocol described in Fig. 1*A*. Mononuclear cell infiltration in the BAL fluid of mice is shown. Data from one experiment are representative of three independent experiments. (*B*) Chemical structures of ascarosides used in the study. (*C*–*G*) Mice were sensitized with synthetic ascarosides (ascr#1, ascr#3, ascr#7, or ascr#10) plus OVA in alum using the same protocol described in Fig. 1*A*. (*C*) Mononuclear cell infiltration in BAL fluid was analyzed 6 d after the OVA challenge. (*D*) Antigen-induced leukocyte infiltration into lungs was evaluated using H&E staining. (*E*) Cell surface expression profiles of CD11b and Siglec-F on the cells in lungs from mice treated with ascarosides. (*F*) AHR in response to increasing doses of methacholine was assessed by measuring lung resistance. (*G*) Antigen-induced goblet cell hyperplasia was evaluated by PAS staining. Representative photographic views of the mice sensitized with ascarosides are shown. (*H*) Mice were sensitized with synthetic ascarosides (ascr#1, ascr#7, ascr#9, dasc#1, or pasc#9) plus OVA in alum using the same protocol described in Fig. 1*A*. Mononuclear cell infiltration in the BAL fluid was analyzed 6 d after the OVA challenge. (Scale bars, 100 mm.) Mean values from more than four mice (*A*, *C*, *F*, and *H*) per group are shown with the SD (*A*, *C*, and *H*) or SEM (*F*). $*P < 0.05$, $**P < 0.01$.

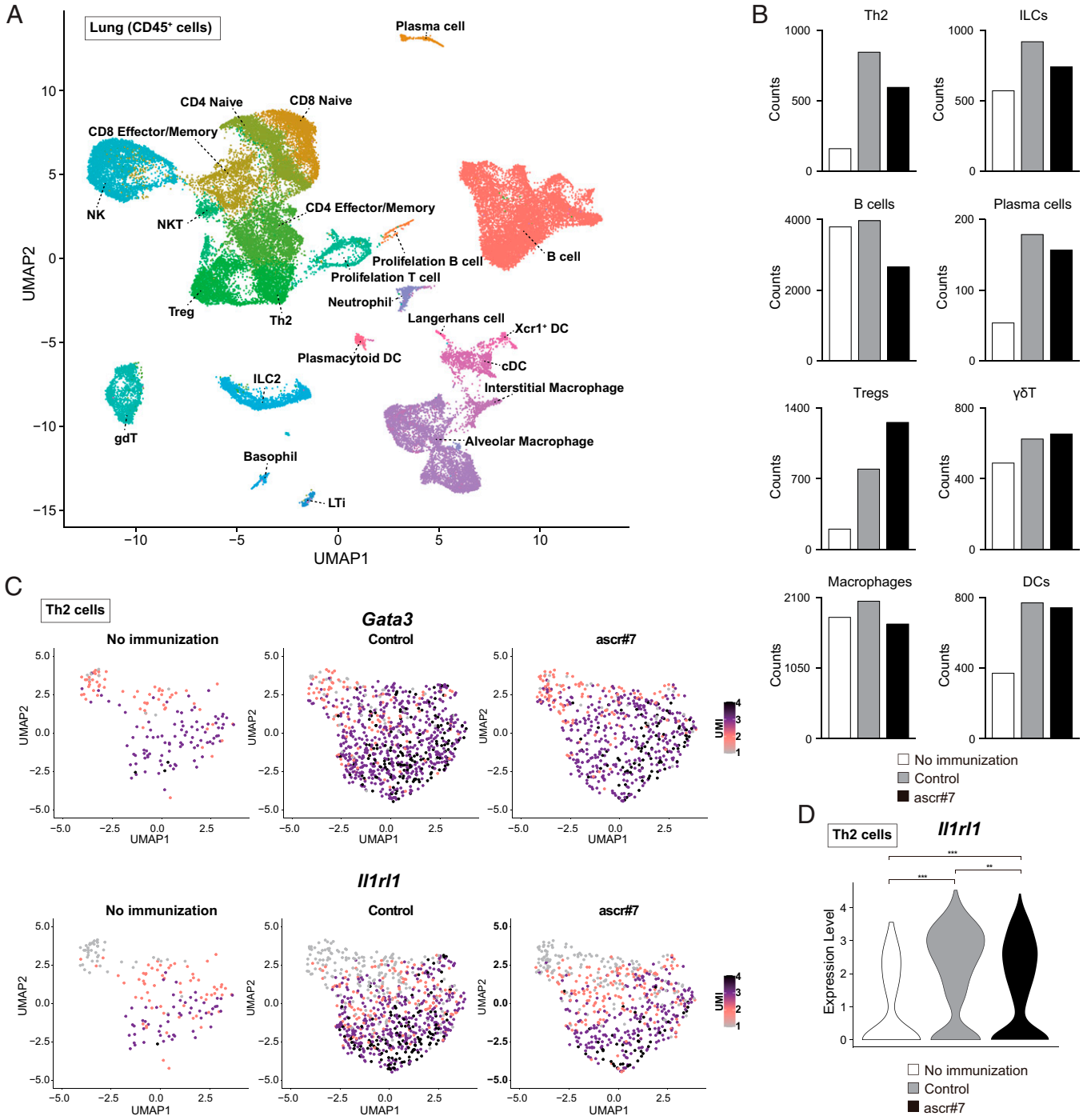

Fig. 3. Ascr#7 decreases the number of ST2^{hi} Th2 cells. (*A*) Single-cell transcriptomes of libraries from lungs of control mice or mice treated with synthetic ascr#7 were projected onto a UMAP of the scRNA-seq libraries from lungs of control mice or mice treated with ascr#7, as indicated in Fig. 1*A*, and colored according to cellular subset. (*B*) Absolute numbers of each cellular subset by treatment condition. White bars indicate cells of mice without immunization (no immunization). Gray bars indicate cells of mice treated with OVA/alum (control). Black bars indicate cells of mice treated with OVA/alum plus ascr#7 (ascr#7). (*C*) Expression of *Gata3* (*Upper*) and *Il1rl1* (*Lower*) projected onto a UMAP. (*D*) Expression of *Il1rl1* projected onto violin plots. $^{**}P < 0.01$, $^{***}P < 0.001$; UMI, unique molecular identifiers.

day 15 (Fig. 4*A*). Moreover, numbers of memory-type ST2$^+$ Th2 cells (CD44$^+$ST2$^+$ CD4 T cells) in lungs of mice that received ascr#7 during the priming phase were also significantly decreased on day 24 (Fig. 4*B* and *SI Appendix*, Fig. S5*B*). The production of Th2 cytokines, particularly IL-4 and IL-5, in lung-infiltrated CD4 T cells from mice that received ascr#7 was also significantly decreased, without any evident switch to IFN-γ (Fig. 4*C*). At the same time, the ability of lung ST2$^+$ Th2 cells to produce Th2 cytokines was attenuated in mice that received ascr#7 at priming (Fig. 4*D*). Furthermore, a marked reduction in the number of ILCs (Fig. 4*E*), particularly GATA3-expressing ILC2s (Fig. 4*F*), was observed in the lungs of mice that received ascr#7 at priming. However, the percentages of IL-5– and IL-13–producing cells in the ILC compartment in

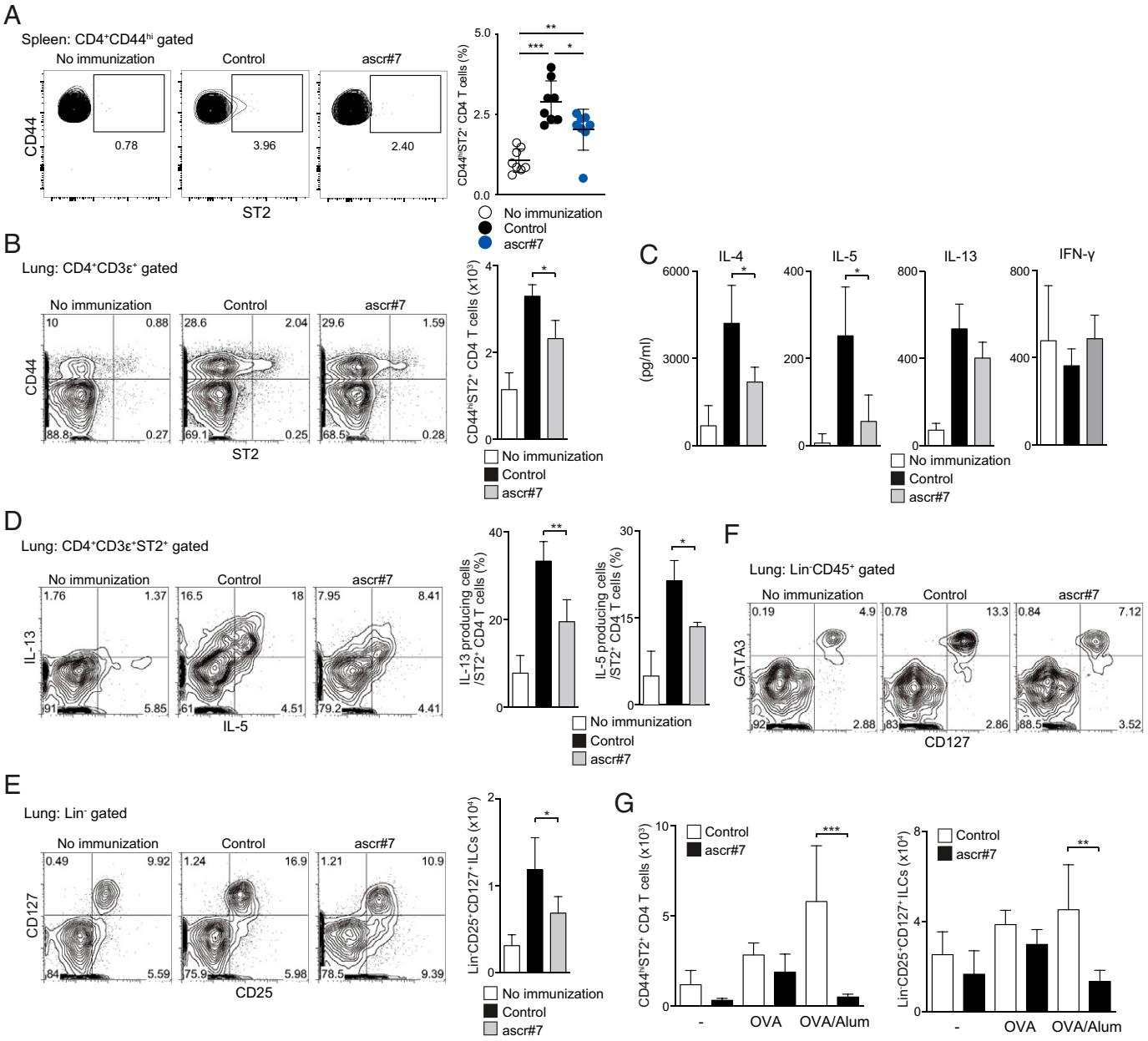

Fig. 4. Priming with ascr#7 attenuates both innate and adaptive type 2 immunity in the lung. Mice were sensitized with synthetic ascr#7 plus OVA in alum on days 0 and 14, and indicated assays were performed on day 15 as described in *SI Appendix*, Fig. S2*A*. (*A*) Representative staining profiles of CD44 and ST2 expression on $CD4^+CD44^{hi}$ cells from spleen (*Left*) and percentages of $CD44^{hi}ST2^+CD4^+$ T cells in the spleen (*Right*). Data from one experiment are representative of two independent experiments (*Left*) and pooled from two independent experiments (*Right*). Mean values from eight mice per group are shown with SD. $*P < 0.05$, $**P < 0.01$, $***P < 0.001$. Mice were sensitized with synthetic ascr#7 plus OVA in alum on days 0 and 14, and indicated assays were performed on day 24 as described in *SI Appendix*, Fig. S2*B*. (*B*) Representative staining profiles of CD44 and ST2 expression on $CD3e^+CD4^+$ cells from lungs (*Left*) and absolute cell numbers of $CD44^{hi}ST2^+CD3e^+CD4^+$ T cells in lungs (*Right*). (*C*) Lung $CD3e^+CD4^+$ T cells from mice sensitized with ascr#7 or with control (solvent vehicle) were prepared and stimulated subsequently in vitro with OVA and APCs. An ELISA measured the indicated cytokines in the culture supernatants collected after 72 h. Mean values with SD are shown. (*D*) Lung mononuclear cells were isolated from mice sensitized with ascr#7 or control (solvent vehicle) and stimulated with anti-TCRb mAb for 6 h. Representative intracellular staining profiles of IL-5 and IL-13 gated on $CD4^+CD3e^+ST2^+$ cells are shown (*Left*). Percentages of IL-13– or IL-5–producing cells in $CD4^+CD3e^+ST2^+$ cells are shown (*Right*). (*E*) Representative staining profiles of CD25 and CD127 expression on lineage$^-$ (Lin^-) cells of lung mononuclear cells are shown (*Left*). Absolute cell numbers of Lin^- $CD25^+CD127^+$ cells in the lung are shown (*Right*). (*F*) Representative staining profiles of CD127 and intracellular GATA3 expression in Lin^-CD45^+ cells of lung mononuclear cells are shown. (*G*) $CD45^-PECAM^-EpCAM^+$ cells were sorted from the lungs of immunized mice, and qRT-PCR of *Il33* and *Tslp* was performed. Mean values from three (*G*) per group are shown with SD. $*P < 0.05$, $**P < 0.01$.

these mice were not reduced, indicating that the function of the ILC2s was normal on a per-cell basis (*SI Appendix*, Fig. S5*D*).

After allergen challenge, the numbers of both $ST2^+$ Th2 cells and ILC2s were reduced in mice that received ascr#7 at priming, which was consistent with the results of the scRNA-seq analysis (Fig. 4*G* and *SI Appendix*, Fig. S5 *C* and *E*). The percentage of IL-5– and IL-13–producing ILCs in the lungs of mice primed with OVA plus ascr#7 or OVA/alum plus ascr#7 was not altered, even after antigen challenge (*SI Appendix*, Fig. S5*F*). These data indicate that

ascr#7 suppresses both innate and adaptive type 2 immunity in vivo.

Ascr#7 Treatment Modulates Several Pathways that Suppress Type 2 Immunity In Vivo. To clarify the molecular mechanisms through which ascr#7 decreased the number of $ST2^{hi}$ Th2 cells, we investigated the effect of ascarosides on CD4 T cell proliferation and effector T cell differentiation in vitro. Upon antigen stimulation, the division of antigen-specific CD4 T cells was not affected by the administration of ascarosides (*SI Appendix*, Fig. S6*A*). The cytokine (IL-4 and IFN-γ) production profiles of in vitro differentiated Th1/Th2 cells were also not affected by the administration of ascarosides (*SI Appendix*, Fig. S6*B*). These data indicate that ascarosides do not directly modulate antigen-induced CD4 T proliferation and Th1/Th2 cell differentiation.

IL-33 stimulates both pathogenic Th2 (Tpath2) cells and ILC2s and exacerbates their role in allergic airway inflammation (17, 18). Therefore, we next assessed *Il33* expression in airway epithelial cells, which are the major lung IL-33 producers (19). Expression of *Il33* was strongly decreased in lung $EpCAM^{+}CD45^{-}$ epithelial cells from mice that had received ascr#7 at priming, whereas *Tslp* expression was not decreased (Fig. 5*A*). Suppression of IL-33 production was also evident in the serum of mice that received ascr#7 at priming (Fig. 5*B*). Furthermore, the expression of *Il33* and *Tslp* in lung epithelial cells was decreased in mice that received ascr#7 at priming after allergen challenge (*SI Appendix*, Fig. S6*C*). Neuronally derived signals such as the neuropeptide neuromedin U (NMU) play a central role in the activation and proliferation of ILC2s (20). Interestingly, our scRNA-seq datasets (Fig. 3*A*) showed decreased expression of the NMU receptor 1 (*nmur1*) on ILC2s from ascr#7-treated mice (*SI Appendix*, Fig. S6*D*).

Finally, to investigate the effects of ascr#7 on macrophages and dendritic cells (DCs) in the lung, we analyzed our scRNA-seq datasets from mice treated with ascr#7 (Fig. 3*A*). We found that interstitial macrophages were increased by ascr#7 administration (Fig. 5 *C* and *D*). Furthermore, the *Il10*-expressing subpopulation of interstitial macrophages was increased in lungs of ascr#7-treated mice (Fig. 5 *E* and *F*). Indeed, fluorescence-activated cell sorting (FACS) analysis revealed increased production of IL-10 by $CD11b^{+}CD64^{high}$MHC class II^{+} interstitial macrophages from ascr#7-treated mice (Fig. 5*G* and *SI Appendix*, Fig. S6*E*). Taken together, these data indicate that ascr#7 is involved in several molecular mechanisms that suppress type 2 immunity in vivo.

Discussion

We here show that ascr#7, a nematode-specific small molecule, inhibits the development of allergic airway inflammation through the suppression of ILC2s and $ST2^{+}$ Th2 cells. Coadministration of antigen/alum with ascr#7 compromised the IL-33 expression in lung epithelial cells and inhibited the IL-33–mediated proliferation of $ST2^{+}$ Th2 cells and ILC2s. Ascr#7 and the chemically closely related ascr#1 are produced by several mammalian parasitic nematode species, and their presence in ES products from these species may contribute to their beneficial immunomodulatory effects in diverse allergic and autoimmune disorders. The high potency of ascr#7—nanogram quantities were sufficient to suppress asthma in our mouse model—suggests that its activity is derived from interaction with a specific receptor(s), in a manner that may be related to the perception of other pathogen-associated molecular patterns, e.g., flagellin (21).

Naive CD4 T cells differentiate into effector T cells upon stimulation by antigens. The cytokines present in the environment determine which effector T cells are induced, such as Th1, Th2, or Th17 cells (22). In an OVA-induced allergic airway inflammation model, Th2 cells are induced by sensitization with OVA and alum injection. Among Th2 cells, the memory-type IL-5–producing Th2 cell population plays key roles in shaping the pathophysiology of allergic airway inflammation (23). The IL-5–producing subpopulation of Th2 cells is characterized by its expression of ST2, a component of the IL-33 receptor, which is encoded by *Il1rl1* (17). Memory-type Th2 cells that reside in the lung are sufficient to induce asthmatic symptoms and represent key drivers of lung allergic responses (24–26). In addition to acquired Th cell immunity, recent studies have identified another innate cell lineage, ILC2s, as potent Th2 cytokine producers involved in the allergic immune response (18, 27). ILC2s lack antigen-specific receptors and express high levels of an array of cytokine receptors, including IL-25R (IL-17RB), IL-33 (ST2), IL-7Ra, and IL-2Ra (28). ILC2s can rapidly elicit large amounts of IL-5 and IL-13 in response to IL-25 and IL-33 stimulation in the presence of IL-7 and IL-2 (29). Both $ST2^{+}$ Th2 cells and ILC2s are activated by IL-33, and ascr#7 treatment resulted in a decreased amount of IL-33 in inflamed mouse lungs (Fig. 5 *A* and *B*). These data indicate that ascr#7 perception at the parasite–host interface interferes with epithelial IL-33 production, preventing this early alarm signal from activating downstream effectors, including pathogenic memory Th2 cells and ILC2s, which play important roles in both the pathogenesis of allergic airway disease and the immune response against helminths (19). Thus, ascr#7 may abrogate the development of allergic airway disease and possibly other IL-33–driven diseases, as the signaling cascades regulating helminth expulsion and autoimmune disease overlap. In addition, induction of Treg cells was increased in mice with attenuated inflammatory responses (Fig. 3*B*), whereas expression of *nmur1* on ILC2s was decreased in ascr#7-treated mice (*SI Appendix*, Fig. S5*D*). At the same time, the subpopulation of interstitial macrophages that expressed *Il10* was increased in the mice treated with ascr#7 (Fig. 5 *C*–*G*). These results indicate that ascarosides affect both CD4 and non-CD4 T cell subsets, thereby leading to the attenuation of allergic immune responses.

There is considerable interest in nematodes and nematode-derived products as novel treatment modalities for immune disorders. However, the use of live nematodes or their proteinaceous secretions is problematic. Intentional infection with nematodes such as hookworms carries significant ethical and disease risks, and proteins have the problems of antigenicity and delivery. In contrast, naturally occurring small molecules with immune modulatory properties, such as ascarosides, may make desirable pharmacological agents, given that more than half of all currently prescribed drugs are derived from natural products (30). Ascarosides are chemically stable (11), are not metabolized quickly by bacteria (16), and are nontoxic at concentrations present in *C. elegans* extracts (31), which are much higher than the dosages used here to inhibit allergic airway disease. Given that IL-33 appears to play a significant role in inflammation and immune dysregulation (32), ascr#7 may have potential utility for treating a broad range of diseases.

Our results expand the range of nematode-interacting organisms that respond to ascarosides to include mammals, in addition to fungi and plants (13, 14). Therefore, ascarosides, which were identified originally as *C. elegans* pheromones, appear to comprise an evolutionarily conserved molecular signature of nematodes that is broadly recognized among eukaryotes. The finding that ascarosides modulate the mammalian immune system may shed light on the coevolution of nematodes and mammals and, moreover, opens the door to develop new types of small molecule-based tools to probe mammalian immune regulation.

Materials and Methods

Mice. C57BL/6 mice were purchased from CLEA Japan, Inc. For all experiments, the mice were used at 6 to 12 wk of age. OVA-specific T cell receptor αβ transgenic (OT-II Tg) mice were maintained under specific pathogen-free conditions (33). All animal experiments were approved by the Chiba University Review Board for Animal Care.

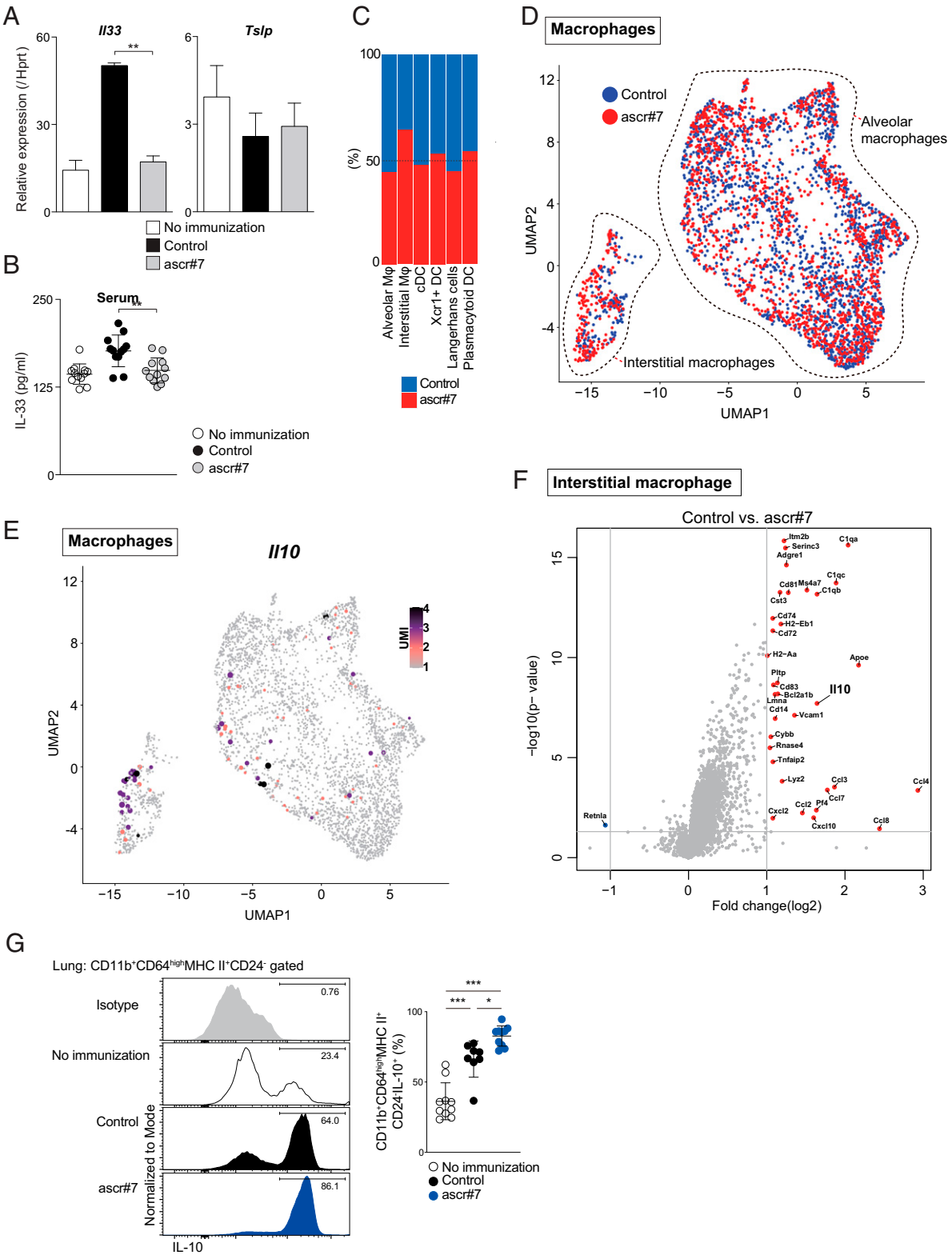

Fig. 5. Ascr#7 suppresses type 2 immunity in vivo. (*A*) CD45$^-$PECAM$^-$EpCAM$^+$ cells were sorted from lungs of immunized mice, and qRT-PCR of *Il33* and *Tslp* was performed. (*B*) Serum IL-33 levels in mice were measured by ELISA. (*C*) Proportion of macrophages and dendritic cells in clusters of alveolar macrophages, interstitial macrophages, cDCs, Xcr1$^+$ DCs, Langerhans cells, and plasmacytoid DCs. (*D*) Expression of macrophages selected from the original dataset projected onto a UMAP. (*E*) Expression of *Il10* projected onto a UMAP. (*F*) This volcano plot depicts differential gene expression following administration of ascr#7 compared to control interstitial macrophages. Mice were sensitized with synthetic ascr#7 plus OVA in alum on days 0 and 14, and then challenged with i.n. administration of OVA or PBS. Six days after the challenge, the indicated assays were performed as described in *SI Appendix*, Fig. S5*E*. (*G*) Representative intracellular staining profiles of IL-10 gated on CD11b$^+$CD64^{high}MHC class II$^+$CD24$^-$ cells are shown (*Left*). Percentages of IL-10–producing cells in CD11b$^+$CD64^{high}MHC class II$^+$CD24$^-$ cells are shown (*Right*). Data from one experiment are representative of two independent experiments (*Left*) and pooled from two independent experiments (*Right*). Mean values from at least eight mice per group are shown with SD. *$P < 0.05$, **$P < 0.01$, ***$P < 0.001$.

Sample Preparation of the smES. *N. brasiliensis* parasites were prepared via a method adapted from those of Holland et al. (34) and Trujillo-Vargas et al. (15). In brief, 5,000 infective-stage (L3) larvae were injected subcutaneously into adult Sprague–Dawley rats. Rats were killed 6 d after infection, and adult worms were harvested from the gut. Adult worms were collected in saline using an adaptation of the Baermann apparatus. After five saline washes, worms were preincubated with 0.15 M NaCl containing 1,000 U/mL penicillin and 1 mg/mL streptomycin before incubation in 0.15 M NaCl with 2% glucose, 100 U/mL penicillin, and 100 mg/mL streptomycin for 5 d at 37 °C. The medium was collected and replaced every other day. smES was prepared by filtering through a 3-kDa filter, followed by lyophilization and heat treatment at 100 °C for 30 min. The amount of smES estimated to be secreted by 125 worms over 3 d was 50 mg.

Identification and Synthesis of Ascarosides. Nematode ES products and lyophilized worms of *N. brasiliensis* (adults), *T. suis* (infective larvae), *A. ceylanicum* (adults), *H. polygyrus* (adults), and *T. spiralis* (infective larvae) were analyzed for the presence of known ascarosides using targeted HPLC with tandem mass spectrometry (MS/MS) as described (10, 16). The retention times of ascarosides detected in the analyzed nematode samples were confirmed with authentic synthetic samples. Ascarosides were synthesized as described previously (35, 36).

Immunization Protocols. C57BL/6 mice were sensitized intraperitoneally with a mixture of 2 μg OVA (Sigma-Aldrich) in 4 mg alum (Thermo Fisher Scientific) (days 0 and 14) with 50 μg of smES or 1 μL of 1 mM synthetic ascarosides or solvent vehicle as a control. On day 24, the mice were anesthetized with isoflurane and challenged intranasally with 30 μL phosphate-buffered saline (PBS) containing 100 μg OVA. In some experiments, C57BL/6 mice were sensitized intraperitoneally with a mixture of 2 μg of OVA in 4 mg alum (days 0 and 14). On day 24, the mice were anesthetized with isoflurane and challenged intranasally with 30 μL PBS containing 100 μg OVA with 1 μL of 1 mM ascr#7 or solvent vehicle as a control. To investigate HDM-induced airway inflammation, C57BL/6 mice were anesthetized with isoflurane and administrated 20 μL PBS containing 100 μg HDM (Greer) intranasally and 300 μL of PBS containing 1 μL of 1 mM ascr#7 or solvent vehicle as a control intraperitoneally on days 0, 1, 2, 7, 8, 9, 14, 15, 16.

Measurement of AHR. The AHR was assessed in the mice using methacholine-induced (Sigma-Aldrich) airflow obstruction, as previously described (37). The respiratory parameters were obtained after exposure to 0.9% saline mist, followed by incremental doses of aerosolized methacholine (0, 3, 6, 12, 24, and 48 mg/mL in a saline solution). The AHR was assessed by a computer-controlled small animal ventilator (SCIREQ).

Collection of the BAL Fluid. BAL was obtained 6 d after the last OVA challenge, as described previously (37). All BAL fluid was collected, and the cells were counted in 100-μL aliquots. A total of 1×10^5 viable BAL cells were cytocentrifuged onto slides by a Cytospin4 (Thermo Fisher Scientific) and stained with Diff-Quick (Sysmex). A total of 200 leukocytes were counted for each slide. The cell types were identified using morphological criteria, and the percentages of each cell type were calculated.

Lung Histology. The mice were killed by asphyxiation, and the lungs were infused with 10% (vol/vol) formalin in PBS buffer for fixation. The lung samples were sectioned, stained with hematoxylin and eosin (H&E) or PAS, and examined for pathological changes under a light microscope at 100× magnification.

qRT-PCR. Total RNA was isolated using the TRIzol reagent (Invitrogen). RNA was then reverse transcribed using oligo (dT) primer and SuperScript II (Invitrogen). qRT-PCR was performed using an ABI PRISM 7500 Sequence Detection System (Applied Biosystems). TaqMan probes (Roche) and gene-specific primers (Sigma-Aldrich) were used for the detection, and the expression was normalized to the hypoxanthine-guanine phosphoribosyltransferase (*Hprt*) signal.

Flow Cytometry and Antibodies. Mice were killed by anesthesia and perfused with 5 mL cold PBS through the right ventricle. The lungs were transferred to a tube containing ice-cold digestion buffer (RPMI medium 1640 supplemented with collagenase type III [200 U/mL; Worthington Biochemical] and DNase I [200 μg/mL; Sigma-Aldrich]) and kept at 4 °C until digestion. Individual lungs were dissociated in 3 mL of digestion buffer using a gentleMACS Dissociator (Miltenyi Biotec). This was followed by incubation for 30 min at 37 °C with frequent agitation and finally gentle magnetic-activated cell sorting (MACS) dissociation. Lung mononuclear cells were separated by centrifugation on a Percoll gradient (GE Healthcare). Single-cell suspensions were prepared from the lungs of individual mice. For cell staining, the cells were stained for 20 min at 4 °C with monoclonal antibodies against CD3e (145-2C11), CD4 (RM4-5), CD4 (GK1.5), CD11b (M1/70), CD11c (N418), CD25 (PC61.5), CD45 (30-F11), B220 (RA3-6B2), CD19 (1D3), NK1.1 (PK136), TER119, Ly-6G (RB6-8C5), MHC II (M5/114.15.2), and an isotype control were purchased from Tonbo Biosciences; TCRγδ (GL3), Siglec-F (E50-2440), and Thy1.2 (30-H12) were purchased from Becton Dickinson and Company; and CD44 (IM7), EpCAM (G8.8), CD4 (RM4-5), CD11b (M1/70), CD64 (X54-5/7.1), CD24 (M1/69), and ST2 (DIH9) were purchased from BioLegend. To exclude dead cells, we stained the cells with 1 μg/mL propidium iodide (PI) (Sigma-Aldrich). To assess the cytokine production from innate lymphoid cells (ILCs), lung mononuclear cells were stimulated in vitro with 50 ng/mL phorbol 12-myristate 13-acetate (PMA) (Sigma-Aldrich) plus 500 nM ionomycin (Merck) with 2 mM monensin (Sigma-Aldrich) for 4 h, and cell surface molecules were stained for 20 min at 4 °C. Intracellular staining was performed using the BD Cytofix/Cytoperm Fixation/Permeabilization Solution Kit according to the manufacturer's protocol. Monoclonal antibodies against IL-5 (TRFK5; BioLegend), IL-13 (eBio13A; Thermo Fisher Scientific), and IL-10 (JE55-16E3; BioLegend) were used for intracellular staining. The stained samples were analyzed on a BD FACS CantoII flow cytometer (Becton Dickinson and Company). The flow cytometric data were analyzed using FlowJo software (Tree Star, Inc.).

An Enzyme-Linked Immunosorbent Assay (ELISA) to Measure the Cytokine Concentration. Lung $CD4^+CD3e^+$ cells from the mice immunized with ascr#7 or control (solvent vehicle) were purified with a FACSAria cell sorter (Becton Dickinson and Company). Cells were cultured with OVA plus irradiated splenic antigen-presenting cells (APCs) for 96 h. The supernatants were collected, and the concentrations of IL-4, IL-5, and IFN-γ were measured by an ELISA, as described previously (37). The production of IL-13 was evaluated with a mouse IL-13 ELISA Kit (R&D Systems) according to the manufacturer's protocol.

An ELISA to Measure the Serum IL-33 Concentration. The concentration of IL-33 in serum was evaluated with a mouse IL-33 ELISA Ready-Set-Go Kit (Thermo Fisher Scientific) according to the manufacturer's protocol.

scRNA-Seq. Cells of $CD45^+$ fractions that were freshly prepared from mice conjunctival tissue and sorted using a BD FACS Aria II (10,000 cells each; cell viability >98%) were encapsulated into droplets, and libraries were prepared using Chromium Single Cell 3′ Reagent Kits v3 according to the manufacturer's protocol (10× Genomics). The generated scRNA-seq libraries were sequenced using 128 cycles (paired-end reads) with a NovaSEq 6000 (Illumina).

Statistical Analyses. Data are shown as mean ± SD or mean ± SEM. Statistical analyses were performed using GraphPad Prism (GraphPad Software). Differences were determined using two-tailed Student's *t* tests, Tukey's multiple comparisons tests, one-way analysis of variance with Tukey's multiple comparison, or two-way analysis of variance with Tukey's multiple comparison. A *P* value of <0.05 was considered statistically significant.

Data Availability. All study data are included in the article and/or *SI Appendix*. Additional data is available at the Gene Expression Omnibus at accession number GSE196470.

ACKNOWLEDGMENTS We thank Ellen Rothenberg, Mary Yui, and Sylvia Vetrone for their invaluable discussions and advice. We thank Ed Platzer for his assistance with the smES preparation and Stephan H. von Reuss and Sydney Campbell for analyzing nematode extracts. We also thank Kaoru Sugaya and Toshihiro Ito for their excellent technical assistance. This work was supported by the Ministry of Education, Culture, Sports, Science and Technology (MEXT Japan) Grants-in-Aid for Scientific Research (S) JP19H05650, (B) 20H03685, (C) 17K08876, 18K07164, and 19K16683, Transformative Research Areas (B) JP21H05120, and JP21H05121; JST FOREST Program (JPMJFR200R); Practical Research Project for Allergic Diseases and Immunology (Research on Allergic Diseases and Immunology) from the Japan Agency for Medical Research and Development (AMED) (Nos. JP21ek0410082, JP21ek0410060, and JP19ek 0410045); Japan Agency for Medical Research and Development (AMED)-PRIME, AMED (No. JP20gm6110005); Japan Agency for Medical Research and Development (AMED)-CREST, AMED (No. JP20gm1210003); Mochida Memorial Foundation for Medical and Pharmaceutical Research, MSD Life Science Foundation, the Naito Foundation, and the Takeda Science Foundation. P.W.S. was an investigator of the Howard Hughes Medical Institute, which supported this work. We further acknowledge support from the Atkinson Center for a Sustainable Future (to F.C.S. and J.A.A.), the Triad Foundation (to F.C.S.), and NIH CBI training grant T32GM008500 (to J.S.H.).

1. P. J. Hotez *et al.*, The global burden of disease study 2010: Interpretation and implications for the neglected tropical diseases. *PLoS Negl. Trop. Dis.* **8**, e2865 (2014).
2. R. M. Maizels *et al.*, Helminth parasites–Masters of regulation. *Immunol. Rev.* **201**, 89–116 (2004).
3. J. E. Allen, R. M. Maizels, Diversity and dialogue in immunity to helminths. *Nat. Rev. Immunol.* **11**, 375–388 (2011).
4. R. M. Maizels, M. Yazdanbakhsh, Immune regulation by helminth parasites: Cellular and molecular mechanisms. *Nat. Rev. Immunol.* **3**, 733–744 (2003).
5. M. S. Wilson *et al.*, Suppression of allergic airway inflammation by helminth-induced regulatory T cells. *J. Exp. Med.* **202**, 1199–1212 (2005).
6. D. E. Elliott, R. W. Summers, J. V. Weinstock, Helminths as governors of immune-mediated inflammation. *Int. J. Parasitol.* **37**, 457–464 (2007).
7. J. V. Weinstock, Helminths and mucosal immune modulation. *Ann. N. Y. Acad. Sci.* **1072**, 356–364 (2006).
8. P. K. Mishra, N. Patel, W. Wu, D. Bleich, W. C. Gause, Prevention of type 1 diabetes through infection with an intestinal nematode parasite requires IL-10 in the absence of a Th2-type response. *Mucosal Immunol.* **6**, 297–308 (2013).
9. A. R. Khan, P. G. Fallon, Helminth therapies: Translating the unknown unknowns to known knowns. *Int. J. Parasitol.* **43**, 293–299 (2013).
10. A. Choe *et al.*, Ascaroside signaling is widely conserved among nematodes. *Curr. Biol.* **22**, 772–780 (2012).
11. J. Srinivasan *et al.*, A blend of small molecules regulates both mating and development in Caenorhabditis elegans. *Nature* **454**, 1115–1118 (2008).
12. F. C. Schroeder, Modular assembly of primary metabolic building blocks: A chemical language in C. elegans. *Chem. Biol.* **22**, 7–16 (2015).
13. Y. P. Hsueh, P. Mahanti, F. C. Schroeder, P. W. Sternberg, Nematode-trapping fungi eavesdrop on nematode pheromones. *Curr. Biol.* **23**, 83–86 (2013).
14. P. Manosalva *et al.*, Conserved nematode signalling molecules elicit plant defenses and pathogen resistance. *Nat. Commun.* **6**, 7795 (2015).
15. C. M. Trujillo-Vargas *et al.*, Helminth-derived products inhibit the development of allergic responses in mice. *Am. J. Respir. Crit. Care Med.* **175**, 336–344 (2007).
16. S. H. von Reuss *et al.*, Comparative metabolomics reveals biogenesis of ascarosides, a modular library of small-molecule signals in C. elegans. *J. Am. Chem. Soc.* **134**, 1817–1824 (2012).
17. Y. Endo *et al.*, The interleukin-33-p38 kinase axis confers memory T helper 2 cell pathogenicity in the airway. *Immunity* **42**, 294–308 (2015).
18. K. Moro *et al.*, Innate production of T(H)2 cytokines by adipose tissue-associated c-Kit(+)Sca-1(+) lymphoid cells. *Nature* **463**, 540–544 (2010).
19. H. Hammad, B. N. Lambrecht, Barrier epithelial cells and the control of type 2 immunity. *Immunity* **43**, 29–40 (2015).
20. C. S. N. Klose *et al.*, The neuropeptide neuromedin U stimulates innate lymphoid cells and type 2 inflammation. *Nature* **549**, 282–286 (2017).
21. L. A. O'Neill, D. Golenbock, A. G. Bowie, The history of toll-like receptors - Redefining innate immunity. *Nat. Rev. Immunol.* **13**, 453–460 (2013).
22. Y. Kanno, G. Vahedi, K. Hirahara, K. Singleton, J. J. O'Shea, Transcriptional and epigenetic control of T helper cell specification: Molecular mechanisms underlying commitment and plasticity. *Annu. Rev. Immunol.* **30**, 707–731 (2012).
23. T. Nakayama *et al.*, Th2 cells in health and disease. *Annu. Rev. Immunol.* **35**, 53–84 (2017).
24. K. Shinoda *et al.*, Thy1+IL-7+ lymphatic endothelial cells in iBALT provide a survival niche for memory T-helper cells in allergic airway inflammation. *Proc. Natl. Acad. Sci. U.S.A.* **113**, E2842–E2851 (2016).
25. B. D. Hondowicz *et al.*, Interleukin-2-dependent allergen-specific tissue-resident memory cells drive asthma. *Immunity* **44**, 155–166 (2016).
26. H. Hammad, B. N. Lambrecht, The basic immunology of asthma. *Cell* **184**, 1469–1485 (2021).
27. K. Hirahara, A. Aoki, M. Kiuchi, T. Nakayama, Memory-type pathogenic T_H2 cells and ILC2s in type 2 allergic inflammation. *J. Allergy Clin. Immunol.* **147**, 2063–2066 (2021).
28. M. Salimi *et al.*, A role for IL-25 and IL-33-driven type-2 innate lymphoid cells in atopic dermatitis. *J. Exp. Med.* **210**, 2939–2950 (2013).
29. H. Kabata, K. Moro, S. Koyasu, The group 2 innate lymphoid cell (ILC2) regulatory network and its underlying mechanisms. *Immunol. Rev.* **286**, 37–52 (2018).
30. D. J. Newman, G. M. Cragg, Natural products as sources of new drugs over the last 25 years. *J. Nat. Prod.* **70**, 461–477 (2007).
31. S. E. Kim *et al.*, Crude extracts of Caenorhabditis elegans suppress airway inflammation in a murine model of allergic asthma. *PLoS One* **7**, e35447 (2012).
32. C. Hardman, G. Ogg, Interleukin-33, friend and foe in type-2 immune responses. *Curr. Opin. Immunol.* **42**, 16–24 (2016).
33. M. J. Barnden, J. Allison, W. R. Heath, F. R. Carbone, Defective TCR expression in transgenic mice constructed using cDNA-based alpha- and beta-chain genes under the control of heterologous regulatory elements. *Immunol. Cell Biol.* **76**, 34–40 (1998).
34. M. J. Holland, Y. M. Harcus, P. L. Riches, R. M. Maizels, Proteins secreted by the parasitic nematode Nippostrongylus brasiliensis act as adjuvants for Th2 responses. *Eur. J. Immunol.* **30**, 1977–1987 (2000).
35. N. Bose *et al.*, Complex small-molecule architectures regulate phenotypic plasticity in a nematode. *Angew. Chem. Int. Ed. Engl.* **51**, 12438–12443 (2012).
36. C. Pungaliya *et al.*, A shortcut to identifying small molecule signals that regulate behavior and development in Caenorhabditis elegans. *Proc. Natl. Acad. Sci. U.S.A.* **106**, 7708–7713 (2009).
37. K. Hirahara *et al.*, Repressor of GATA regulates TH2-driven allergic airway inflammation and airway hyperresponsiveness. *J. Allergy Clin. Immunol.* **122**, 512–20.e11 (2008).